

RSC Advances



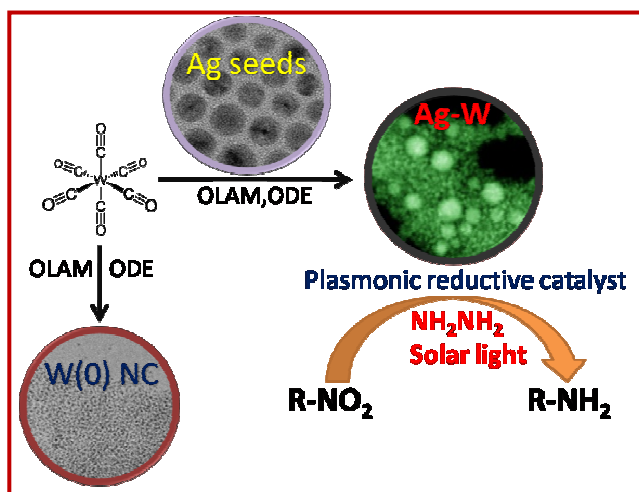
This is an *Accepted Manuscript*, which has been through the Royal Society of Chemistry peer review process and has been accepted for publication.

Accepted Manuscripts are published online shortly after acceptance, before technical editing, formatting and proof reading. Using this free service, authors can make their results available to the community, in citable form, before we publish the edited article. This *Accepted Manuscript* will be replaced by the edited, formatted and paginated article as soon as this is available.

You can find more information about *Accepted Manuscripts* in the [Information for Authors](#).

Please note that technical editing may introduce minor changes to the text and/or graphics, which may alter content. The journal's standard [Terms & Conditions](#) and the [Ethical guidelines](#) still apply. In no event shall the Royal Society of Chemistry be held responsible for any errors or omissions in this *Accepted Manuscript* or any consequences arising from the use of any information it contains.

Ag-W bimetallic plasmonic heterostructures were synthesized with tunable LSPR property in full solar spectrum region and exploited in reduction catalytic process driven by light energy.



COMMUNICATION

Fabrication of Tungsten Nanocrystals and Silver-Tungsten Nanonets: a Potent Reductive Catalyst

Cite this: DOI: 10.1039/x0xx00000x

Sirshendu Ghosh,^a Saikat Khamarui^b, Manas Saha^a and S. K. De^{*a}Received 00th January 2012,
Accepted 00th January 2012

DOI: 10.1039/x0xx00000x

www.rsc.org

This communication reports the first synthesis of well defined colloidal W Nanocrystals, Ag-W heterostructures and their broad plasmon absorbance from visible to near infrared region. Strong interparticle plasmonic interaction significantly improves the photocatalytic reduction performance of silver-tungsten heterostructure.

Nanometals have attracted the researchers for their unique physical and chemical properties¹. Among the various types of physiochemical properties, Localised Surface Plasmon Resonance (LSPR) of metal nanocrystals (NCs) which arises from the collective oscillation of free electron on metal surface coupled with electromagnetic wave is an intriguing phenomenon. The LSPR has the highest interest in present and already applied in different fields including plasmonic based light harvesting process, non-linear optics, bio sensing, surface enhanced Raman spectra, photo catalysis and high speed photo voltaic (PV) solar cell². Plasmonic features in metal NCs can be tuned in visible-near infrared (VIS-NIR) region by regulating the size^{3a,b}, shape^{3c-e}, degree of alloying^{3f-h} or by heterostructure formation^{3i-l}. High energy ultraviolet (UV) plasmon bands of coinage metal NCs (Au, Ag, Cu) are rarely reported for their instability in small dimension, rapid degradation of plasmon band and predominance of interband transition. Recently⁴ high energy plasmon band tuneable up to low energy region was found for aluminium nanocrystals but it faced instability in ambient condition for formation of Al₂O₃ thin layer over the surface of NCs. Some theoretical and experimental studies revealed that the less noble metals (such as In, W, Ga, Sn, Pb, Bi) might show interesting plasmonic properties⁵ and application in plasmonic based catalysis. Tungsten nanoparticles have gained attention mainly due to its widespread applications such as light emitting source^{6a}, hard materials^{6b}, thermionic cathodes, high power batteries and catalysis^{6c} etc. Tungsten exists in two crystalline form α and β (where α is the more stable phase). High oxophilicity of W makes the synthesis of free standing well defined W(0) NCs very difficult. In some recent studies W(0) NCs have been synthesized by thermal decomposition process, using ionic liquid^{7a}, hazardous reduction process^{7b}, sonochemical methods^{7c}, reduction of WO₃^{7d} or chemical vapor deposition^{7e}. But in most cases non-uniform particle distribution or non-crystalline amorphous nanoparticles were found.

Theoretically calculated plasmonic absorbance band of spherical shaped 10 nm W(0) NCs was found at 310 nm⁸ and it is

expected that the band position can be tuned in UV-VIS region by changing size, shape, alloying or by heterostructure formation. For the high oxophilic nature of tungsten ($E_0 = -1.1$ V, NHE for $W^{+6} \rightarrow W^0$), it is capable to reduce the organic nitro compounds having suitable reduction potential value (say, E^0 for Nitro Benzene/Aniline = 0.42 V, NHE) from thermodynamical point of view. Many of non-plasmonic transition metals like Pd, Pt, and Ni show catalytic activity in chemical reactions and in most of the cases they are driven by conventional heating process which may have some negative effect like formation of unwanted product. So the synthesis of a heterostructured or alloy NC containing a plasmonic metal with catalytically active transition metal is important as it could effectively harvest the light energy through the plasmonic absorption and can increase the catalytic ability of transition metal without the heat treatment.

Noble metal nanoparticles (Ag, Au) exhibit good photocatalytic reduction⁹ by their surface plasmon resonance (SPR) effect driven by sun light. In terms of available energy, Visible (43%) and Infrared (52%) light constitute most of the solar emission with very low amount of UV (4%) light¹⁰. The most important photocatalysis challenge is to fabricate new photocatalysts that can absorb large amount of solar energy keeping its activity or specificity intact in ambient condition. Plasmonic coupling among metal nanoparticles generates broad, tuneable plasmon band for different plasmon modes (capacitive, charge transfer) with enhanced electromagnetic field (EM) of course depending upon the degree of contact between two nanostructures¹¹. This enhancement in EM field also increases the photonic absorbance efficiency in wide region of solar spectrum and might boost up the reduction activity. The interaction of visible light with the plasmon resonance of metal nanoparticles can be controlled by proper combination of dissimilar metals. Experimental and theoretical investigations indicate that electromagnetic interaction between metallic nanoparticles is a complex function of size, inter-particle distance, composition and environment. In this communication, objective is twofold: (i) synthesis and optical characterization of W nanoparticles (ii) introduction of plasmonic coupling in random assemble of W and Ag nanoparticles to modify optical absorption spectrum of individual metallic nanoparticle and maximising the catalytic reduction property of W nanocrystals. Plasmonic absorption of W and Ag lies in wavelength region of 300-400 nm. A large difference in

electronegativity between W(2.36) and Ag(1.93) may also play important role to influence plasmonic coupling between metal nanoparticles. The above facts stimulated us to design W-Ag nanonets for better photocatalytic activity at room temperature.

W(0) NCs were synthesized by thermal decomposition of tungsten hexacarbonyl $[W(CO)_6]$ at high temperature in non-polar solvent 1-octadecene (ODE) using Oleylamine (OLAM) as activating and stabilising agent. In a typical synthesis, 1 mM of $W(CO)_6$ and 0.4 mM OLAM were dispersed in 5 ml octadecene (ODE), vacuumed at room temperature for 1 hr and the system was backfilled with dry Ar. The temperature of the reaction flask was slowly increased to 300 °C (10 °C/min) and reaction was continued for 2 hrs. Fig. 1(A) shows the large area TEM image of loosely aggregated W(0) NCs. Fig. 1(C) depicts the closer view of an assembly of NCs with a size of 4 ± 0.5 nm. A high resolution TEM image (Fig. 1D) shows lattice fringes of 0.235 nm corresponding to the (111) plane of fcc tungsten.

Fig. 1(E) shows the XRD pattern of as-synthesized W(0) NCs and the diffraction peaks observed at 37.23, 68.11, 83.21 correspond to (111), (200) and (220) planes of the fcc (α) phase (JCPDF No. 882339). The crystallite size calculated from XRD using Scherer formula is 3.6 nm and comparable well with the TEM result.

The synthesis of W(0) NCs from $W(CO)_6$ complex involved gradual decomposition of metal carbonyl complex and catalysis by the solvent and surfactant molecule. Decomposition of $W(CO)_6$ at high temperature (~ 350 °C) in presence of octadecane and octadecylamine (the saturated form of ODE and OLAM) does not generate crystalline W(0) NCs. Fig. S1 shows the FTIR spectra of OLAM, ODE and OLAM- $W(CO)_x$ and ODE- $W(CO)_x$ intermediate complex. The disappearance of olefinic C-H bond stretching frequency at 3008 cm^{-1} and 3077 cm^{-1} (for OLAM and ODE respectively) of intermediate complexes suggests a ' π ' donation of OLAM and ODE to the metal centre¹². A red shifting and broadening of N-H stretching band at 3336 cm^{-1} of OLAM are observed in OLAM- $W(CO)_x$ intermediate. An increase in intensity and broadening of the C-N stretching band at 1068 cm^{-1} also suggest the involvement of lone pair of OLAM in complex formation¹³. Heating the precursor in octadecane with OLAM also generates W(0) cluster but the synthetic procedure creates high amount of sublimation at temperature ~ 80 °C to 120°C resulting a large loss of reactants. But decomposition in ODE decreases the degree of sublimation by forming complex between $M(CO)_x$ - π bond. The decomposition of $W(CO)_6$ in ODE results in W(0) NCs but with high degree of agglomeration and polycrystalline nature which proves the faith of using OLAM as capping agent (Fig. S2). Use of

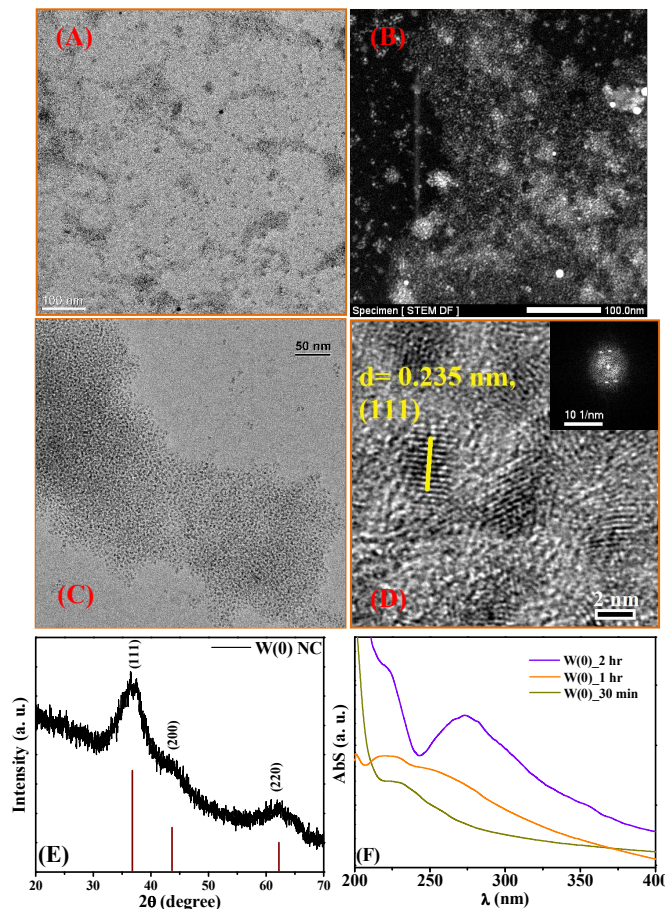


Fig. 1 (A) and (B) are TEM and STEM images of free standing nearly monodispersed W(0) NCs over the large area respectively. (C) A closer View of W(0) NCs assembly. (D) HRTEM image of few NCs and inset shows the corresponding FFT pattern. The major growth plane was found to be (111). (E) XRD pattern of bcc W(0) NCs. (F) Time dependent absorbance spectra of W(0) NCs.

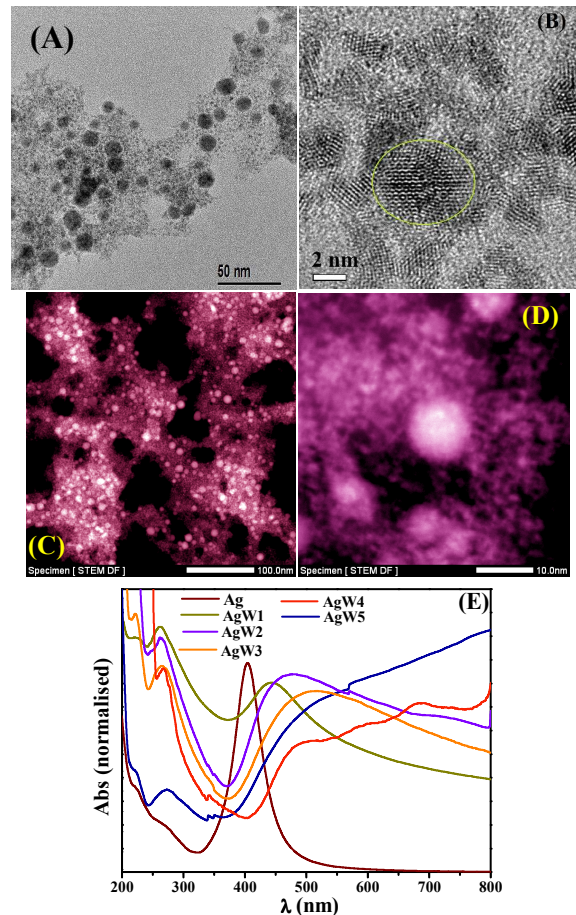


Fig. 2 (A) TEM image of AgW₅ nanonets. (B) HRTEM image AgW₅ shows the presence of W(0) on Ag NC's surface and also in close vicinity. (C) STEM image of nanonet structure shows the formation network over micrometer region and presence of Ag NCs (bright spot) without self agglomeration. (D) Presence of W(0) network around the Ag NCs and connecting another neighbor Ag NC. (E) Normalized absorbance spectra of different AgW₅ heterostructures.

oxygen containing capping agent which contains oxygen at binding group like oleic acid, stearic acid, octadecanol or trioctyl phosphine oxide (frequently used in colloidal synthesis) generates WO_{3-x} NCs (ESI, Fig.S3).

The growth of W(0) free standing NCs was studied by quenching the reaction mixture at different time interval. Fig. S4 shows TEM images of the sample at 5, 15, 30 and 60 min of reaction. Formation of very small sized cluster (~1~1.5 nm) was found in 5 min and 15 min reaction product. The as-formed cluster further grows and TEM image of 30 min product shows the cluster size ~ 2 nm with no such detectable crystalline phase. Crystallinity of the NC was found to be appearing after 1 hr of reaction. The absorbance spectra of the product at different time interval in Fig. 1(F) shows the presence two types of absorbance in each set. The absorbance at 227 nm is believed to be for the OLAM. This absorbance band is found to be blue shifted (~30 nm) than the pure OLAM (250 nm-270 nm, Fig. S5) which indicates the electron donation of the lone-pair at the nitrogen atom of OLAM to the metal surface. Another absorbance band at longer wavelength was found to be red shifted on progress of reaction and shows a strong localised surface plasmon resonance band centred at 273 nm for 2 hr of reaction product extends up to blue region. Previously *Creighton et al*⁸ predicated a plasma band at 310 nm for 10 nm spherical W colloids. Such a blue shift of LSPR band is due to the particle size in quantum confinement region frequently observed for noble metal NCs^{3a}.

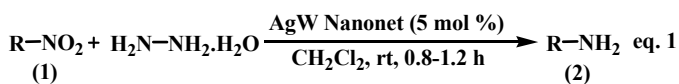
Ag-W nanonets (NNs) were synthesized by employing spherical monodispersed Ag NC (Size 9.6 ± 1.7 nm, ESI, Fig. S6) as the seed material and was employed at the beginning of the reaction. Different compositions of Ag-W NNs have been synthesized by varying the Ag:W molar ratio. For Ag:W =2:1(AgW1), formation of W(0) NCs was found onto the surface of Ag NCs (Fig. S7). Reaction mixture quenched at 280 °C shows presence of an amorphous shell around the free standing Ag NCs (ESI, Fig. S7B). OLAM which was present on the Ag NC's surface as capping agent might be involved in the complex formation with $W(CO)_6$. The amorphous moiety converted to crystalline W(0) NCs upon completion of reaction at 300 °C for 2 hrs. Here heterogeneous nucleation of W(0) onto solid Ag crystalline surface is favoured over homogeneous process in solution as the former one has lower Gibbs energy¹⁴(ΔG) for minimal lattice constant mismatch between Ag and W. Moreover, the presence of OLAM on surface gives a platform for intermediate complex formation. When the Ag:W molar ratio was lowered (1:2; AgW2), more surface coverage of Ag seeds by W(0) NCs was found (Fig. S8). The string like W(0) NC was formed on Ag seeds and extended into the solution during the growth process. When more W-precursor (Ag:W = 1:5, AgW5) was employed in the reaction, a crystalline W-network was found to be form keeping the size and shape of Ag NCs intact depicted in Fig. 2 (A-D). The formation of net-like morphology can be interpreted by heterogeneous nucleation followed by a delayed homogenous nucleation process. First W(0) NC is formed along the crystallographic edges of Ag seeds and additional growth of existing W(0) areas on the seeds takes place. As the growth of W(0) is very slow as observed for free standing W(0) synthesis, we believe a delayed homogeneous nucleation was occurred in solution from the reaction between free OLAM and excess $W(CO)_6$ complex. The as-synthesized W(0) seed in solution and W(0) string present on Ag surface undergoes coalescence to form the net like structure. HRTEM image in Fig. 2(D) shows the presence of W (0) NCs on Ag surface and also at the near surface (< 1 nm). Elemental mapping of AgW nanonets (AgW5) in Fig. S10 confirmed the presence of Ag NCs without self-agglomeration and

W NCs around the Ag moiety and extended network region. Presence of some free standing W(0) NCs (Fig. S8, S10) also supports the delayed nucleation of W(0) in solution.

One important feature of the as-synthesised Ag-W heterostructure is that they exhibit well defined SPR absorbance band and tuneable in total solar spectrum region depending upon the relative amount of Ag and W as demonstrated in Fig. 2(E). Pure Ag NCs which was used as seeds shows a strong plasmon band centred at 404 nm. The absorbance peak maximum is found to be red shifted and broadened when W NCs formed around the surface and gradually forms network. Another plasmon band in UV region 260 nm to 275 nm is appeared for W NCs. The red shift and broadening of Ag plasmonic is not for the morphology change or alloy formation as we found no change in shape of Ag seeds or alloy (AgW) formation from TEM or STEM (element mapping) study. Here plasmonic coupling between Ag and W NCs is expected as W NCs is present on the Ag surface or very close vicinity. The LSPR frequency position of the metal NCs depends on the dielectric constant of dispersion medium. The presence of W NCs change the dielectric environment of Ag NCs by forming heterostructure or nanonets. The dielectric constant value of bulk tungsten is much higher than silver metal^{15a,b}. So W NCs enclosing Ag NCs increases the dielectric constant value of the surroundings of Ag NCs and results a gradual red shift of Ag plasmonic peak as the W concentration increases. The broad peaks for Ag:W NNs mainly composed of 2-3 humps might be the overlap of different plasmon modes such as capacitive plasmon and charge transfer plasmon modes due to random inter-particle distance. The plasmonic sensitivity of the AgW heterostructures is found to be decreased on increasing the W concentration. Fig S13 shows the experimental change of LSPR peak maxima of the NCs/NNs with the refractive index of solvents. Pure Ag NCs shows plasmonic sensitivity ~ 145 nm/RIU and decreases to 79 nm/RIU for AgW5 nanonet sample. The AgW heterostructures (especially AgW nanonets) are very efficient in harvesting the solar light energy (in full solar spectrum) as it contains strong plasmonic band in UV, VIS and NIR region.

The exclusive heterostructure and plasmonic optical properties of the synthesized bimetallic Ag-W composite gives an opportunity to study the light enhanced catalytic applications. The plasmonic property of the synthesized AgW nanonet has been utilized by developing a new reduction method under mild condition. Reduction of nitro group towards amine is a well known chemistry since 1948¹⁶. But the uniqueness of our strategy includes Ag-W catalyzed kinetic acceleration of the reduction process under solar illumination. Aliphatic as well as aromatic nitro compounds (1)

Scheme 1. Plasmonic AgW-nanonet catalyzed reduction acceleration



R = aromatic and aliphatic group

underwent reduction into their corresponding amine functionality (2) in the presence of Ag-W nanonet (5 mol%) and hydrazine hydrate [$N_2H_4 \cdot H_2O$] (1.1 equiv) (eq. 1, Scheme 1).

To compare the catalytic activity among different nanostructures we studied the reduction of p-nitro toluene to p-toluidine in similar reaction condition using the light irradiance of 0.65 Wcm^{-2} (Fig. 3A). The pure Ag NCs was found to be catalytically inactive where W NC shows poor catalysis. Formation

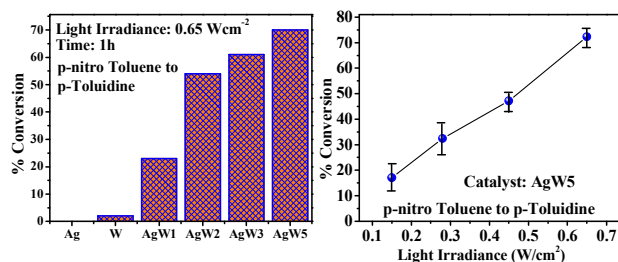
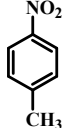
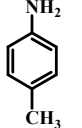
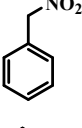
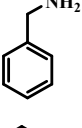
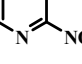
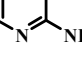
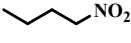
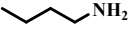
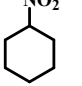
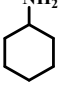
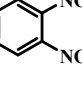
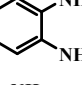
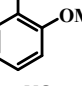
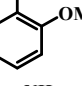
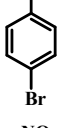
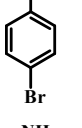
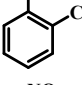
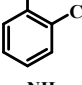
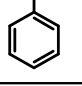
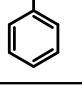


Fig. 3 (A) Catalytic activity of different nanostructures. (B) Dependence of catalytic activity of AgW5 on light irradiance.

Table 1. Substrate scope for the catalytic reduction process

Entry	Starting Material (1)	Product (2)	Time (h)	Yield (%)
1			1.1	2a, 78
2			1.0	2b, 71
3			1.0	2c, 73
4			0.8	2d, 66
5			0.8	2e, 70
6			1.2	2f, 63
7			1.1	2g, 66
8			1.0	2h, 80
9			1.0	2i, 82
10			1.1	2j, 70

of AgW heterostructure was found to be effective and maximum activity was found for AgW5 NN structure which shows maximum plasmonic absorbance in visible and NIR region. To study the dependence of catalytic rate on light irradiance we carried out the

same reaction using AgW5 catalyst at different light irradiance (standardised with a photometer). The almost linear dependence of % conversion with light power density clearly indicates the SPR property of heterostructures plays a vital role in solar light driven catalytic process. For more clear understanding of the catalytic process XPS was performed with the AgW5 catalyst and recovered catalyst after 15 min of reaction (Fig. S14). As synthesized AgW5 catalyst shows two peaks at 31.58 eV and 33.68 eV for W 4f_{7/2} and W4f_{5/2} respectively owing to spin orbit splitting. Recovered catalyst shows four peaks in binding energy range 30-40 eV. Deconvolution results in two peaks at higher energy region 35.62 and 37.63 eV assigned for W⁶⁺ and the lower energy peaks at 31.66 and 33.67 eV correspond to W(0)^{17a,b}. So during the reduction process W(0) might be oxidised to W⁶⁺ state and then reduced back to W(0) by hydrazine.

Optimization study (ESI, Table 1.1) revealed that only 5 mol% of the catalyst is sufficient to perform its activity and commonly used hydrazine is found to be a potential candidate for catalyst regeneration. Under the developed condition, varieties of nitro compounds were screened to illustrate the robustness and generalization of the procedure. Aromatic ring possessing electron donating (entry 1,7 Table 1) and electron withdrawing substituents (entry 6,8,9, Table 1), heterocyclic ring (3), aliphatic analogues (2,4,5) are well tolerated towards valuable amino synthons (2a-j, Table 1). All the structures were confirmed by spectroscopic analyses (ESI) and comparing with the literature. Surprising result was obtained for 1,2-dinitrobenzene (entry 6) as both the nitro group got reduced to *o*-phenelenediamine (2f) very easily. Thus the developed strategy demonstrates a simple, non-hazardous reduction technique with fast reaction convergence.

In Summary, we have successfully synthesized the free standing W(0) NCs by thermal decomposition process and fabricated bimetallic Ag-W heterostructure using Ag seeds with tunable SPR feature. The Ag-W nanonet structure shows efficient reductive photocatalytic activity. High oxophilic W in Ag-W heterostructure acts as catalytic site as evidenced from XPS study. Design of heterostructure comprising of metal nanoparticles is found to be crucial for enhancement of the photocatalytic process.

S.G and M. S acknowledge CSIR, India for providing the fellowship (SRF and JRF) during the tenure of work.

Notes and references

^aDepartment of Materials Science, Indian Association for the Cultivation of Science, Kolkata-700032, India. E-mail: msskd@iacs.res.in; Tel: +91-33-2473-3073. ^b Department of Chemistry, University of Calcutta, University College of Science, 92, A. P. C. Road, Kolkata-700009, India

Electronic Supplementary Information (ESI) available: Experimental procedures, additional characterisation and others. See DOI: 10.1039/c000000x/

- (a) P. K. Jain, X. Huang, I. H. El-Sayed and M. A. El-Sayed, *Acc. Chem. Res.* 2008, **41**, 1578; (b) M. E. Stewart, C. R. Anderton, L. B. Thompson, J. Maria, S. K. Gray, J. A. Rogers and Ralph G. Nuzzo, *Chem. Rev.*, 2008, **108**, 494; (c) S. Linic, P. Christopher, D. B. Ingram, *Nat. Mater.* 2011, **10**, 911 – 921.

- (d) J. A. Schuller, E. S. Barnard, W. S. Cai, Y. C. Jun, J. S. White, M. L. Brongersma, *Nat. Mater.* 2010, **9**, 193 – 204.
2. (a) Y Zakharko, T Nychyporuk, L Bonacina, M Lemiti and V Lysenko, *Nanotechnology*, 2013, **24**, 055703. (b) J. N. Anker, W. P. Hall, O. Lyandres, N. C. Shah, J. Zhao and R. P. V. Duyne, *Nat. Mater.*, 2008, **7**, 442. (c) J-H. Lee, J-M. Nam, K-S. Jeon, D-K. Lim, H. Kim, S. Kwon, H. Lee and Y. D. Suh, *Acs Nano*, 2012, **6**, 9574. (d) P. D. Howes, S. Rana and M. M. Stevens, *Chem.Soc.Rev.*, 2014, **43**, 3835. (e) S. Linic, P. Christopher and D. B. Ingram, *Nat. Mat.*, 2011, **10**, 911. (f) X. Zhang, Y. L. Chen, R-S. Liu and D. P. Tsai, *Rep. Prog. Phys.*, 2013, **76**, 046401. (g) S. Pillai, K. R. Catchpole, T. Trupke and M. A. Green, *J. Appl. Phys.*, 2007, **101**, 093105.
3. (a) J. A. Scholl, A. L. Koh and J. A. Dionne, *Nature*, 2012, **483**, 421. (b) S. Peng, J. M. McMahon, G. C. Schatz, S. K. Gray, and Y. Sun, *Proc. Nat. Aca. Sc.*, 2010, **107**, 14530. (c) H. Chen, L. Shao, K. C. Woo, T. Ming, H-Q. Lin, and J. Wang, *J. Phys. Chem. C*, 2009, **113**, 17691. (d) A. Tao, P. Sinsermsuksakul and P. Yang, *Nat. Nanotech.*, 2007, **2**, 435. (e) B. Nikoobakht and M. A. El-Sayed, *Chem. Mater.*, 2003, **15**, 1957. (f) N. E. Motl, E. Ewusi-Annan, I. T. Sines, L. Jensen and R. E. Schaak, *J. Phys. Chem. C*, 2010, **114**, 19263. (g) R. He, Y-C. Wang, X. Wang, Z. Wang, G. Liu, W. Zhou, L. Wen, Q. Li, X. Wang, X. Chen, J. Zeng and J. G. Hou, *Nat. Comm.*, DOI: 10.1038/ncomms5327. (h) M. P. Mallin and C. J. Murphy, *Nano Lett.*, 2002, **2**, 1235. (i) S. Mandal, PR. Selvakannan, R. Pasricha and M. Sastry, *J. Am. Chem. Soc.* 2003, **125**, 8440. (j) Y. Ma, W. Li, E. C. Cho, Z. Li, T. Yu, J. Zeng, Z. Xie, and Y. Xia, *ACS Nano*, 2010, **4**, 6725. (k) C. Liusman, H. Li, G. Lu, J. Wu, F. Boey, S. Li and H. Zhang, *J. Phys. Chem. C*, 2012, **116**, 10390. (l) O.Pena-Rodríguez, U. Pal, M. Campoy-Quiles, L. Rodríguez-Fernandez, M. Garriga and M. I. Alonso, *J.Phys.Chem.C*, 2011, **115**, 6410.
4. (a) M. W. Knight, N. S. King, L. Liu, H. O. Everitt, P. Nordlander and N. J. Halas, *Acs Nano*, 2014, **8**, 834. (b) M. W. Knight, L. Liu, Y. Wang, L. Brown, S. Mukherjee, N. S. King, H. O. Everitt, P. Nordlander and Naomi J. Halas, *Nano Lett.*, 2012, **12**, 6000.
5. (a) C. Kind and C. Feldmann, *Chem. Mater.*, 2011, **23**, 4982. (b) J. M. McMahon, G. C. Schatz and S. K. Gray, *Phys. Chem. Chem. Phys.*, 2013, **15**, 5415.
6. (a) P. Heszler, L. Landstrom, M. Lindstam, and J. O. Carlsson, *J. Appl. Phys.*, 2001, **89**, 3967. (b) J.C. Bailar, H.J. Emeleus, *Compr. Inorg. Chem.*, 1973, **3**, 742. (c) L. Xiong and T. He, *Chem. Mater.*, 2006, **18**, 2211.
7. (a) E. Redel, R. Thomannb and C. Janiak, *Chem. Commun.*, 2008, 1789. (b) C. Schottle, P. Bockstaller, D. Gerthsen and C. Feldmann, *Chem. Commun.*, 2014, **50**, 4547. (c) H. Lei, Y.-J. Tang, J.-J. Wei, J. Li, X.-B. Li, H.-L. Shi, *Ultrasonics Sonochemistry*, 2007, **14**, 81. (d) H.H. Nersisyan, J.H. Lee, C.W. Won, *Combust. Flame*, 2005, **142**, 241. (e) L. Landstrom, J. Lu and P. Heszler, *J. Phys. Chem. B*, 2003, **107**, 11615.
8. J. A. Creighton and D. G. Eadon, *J. Chem. Soc., Faraday Trans.*, 1991, **87**, 3881.
9. (a) X. Ke, S. Sarina, J. Zhao, X. Zhang, J. Changa and H. Zhu, *Chem. Commun.*, 2012, **48**, 3509. (b) T. Wu, S. Liu, Y. Luo, W. Lu, L. Wanga and X. Sun, *Nanoscale*, 2011, **3**, 2142. (c) D. Kumar, S. Kaur and D.-K. Lim, *Chem. Commun.*, 2014, **50**, 13481.
10. Z. Zou, J. Ye, K. Sayama1 & H. Arakawa1, *Nature*, 2001, **414**, 625.
11. J.-H. Lee, M.-H. You, G.-H. Kim and J.-M. Nam, *Nano Lett.*, 2014, **14**, 6217.
12. (a) S. Ghosh, K. Das, K. Chakrabarti and S. K. De, *Dalton Trans.*, 2013, **42**, 3434. (b) P. J. Thistlethwaite and M. S. Hook, *Langmuir*, 2000, **16**, 4993.
13. S. Ghosh, M. Saha and S. K. De, *Nanoscale*, 2014, **6**, 7039.
14. (a) J. Park, J. Joo, S. G. Kwon, Y. Jang, and T. Hyeon, *Angew. Chem., Int. Ed.*, 2007, **46**, 4630. (b) E. E. Finney, R. G. Finke, *J. Colloid Interface Sci.* 2008, **317**, 351.
15. (a) L. V. Nomerovannaya, M. M. Kirillova and M. M. Noskov, *Soviet Physics JETP.*, 1971, **33**, 405. (b) P. B. Johnson and R. W. Christy, *Phys. Rev. B*, 1972, **6**, 4370.
16. J. Pearson, *Trans. Faraday Soc.*, 1948, **44**, 683.
17. (a) J. Li, Y. Liu, Z. Zhu, G. Zhang, T. Zou, Z. Zou, S. Zhang, D. Zeng and C. Xie, *Sci. Rep.*, 2013, **3**, 2409. (b) N. V. Alov, *J. Anal. Chem.*, 2005, **60**, 431.